A Bayesian Approach of Hyperanalytic Wavelet Transform Based Denoising

Ioana Adam[1], Corina Nafornita[1], Jean-Marc Boucher[2], Alexandru Isar[1]
[1] Communications Dept., Electronics and Telecommunications Faculty, "Politehnica" University, Timisoara, Romania
ioana.adam@etc.upt.ro, corina.nafornita@etc.upt.ro, alexandru.isar@etc.upt.ro
[2] Dept. SC, GET, ENST Bretagne, CNRS, Brest, France
jm.boucher@enst-bretagne.fr

Abstract **– The property of shift-invariance associated with a good directional selectivity is important for the application of a wavelet transform, (WT), in many fields of image processing. Generally, complex wavelet transforms, like for example the Double Tree Complex Wavelet Transform, (DTCWT), have these good properties. In this paper we propose the use of a new implementation of such a WT, recently introduced, namely the hyperanalytic wavelet transform, (HWT), in denoising applications. The proposed denoising method is very simple, implying three steps: the computation of the forward WT, the filtering in the wavelets domain and the computation of the inverse WT, (IWT). The goal of this paper is the association of a new implementation of the HWT, recently proposed, with a maximum a posteriori (MAP) filter. Some simulation examples and comparisons prove the performances of the proposed denoising method.**

Keywords **– Directional selectivity, Hyperanalytic wavelet transform, Image denoising, Maximum a posteriori filter.**

I. INTRODUCTION

During acquisition and transmission, images are often corrupted by additive noise that can be modeled as Gaussian most of the time. The aim of an image-denoising algorithm is then to reduce the noise level, while preserving the image features. Such a system must realize a big noise reduction in the homogeneous regions and the preservation of the details of the scene in the other regions. There is a big diversity of estimators used as denoising systems. One may classify these systems in two categories, those, which are directly applied to the signal, and those, which use a wavelet transform before processing. In fact, David Donoho, introduced the word denoising in association with the wavelet theory, [1]. From the first category, taking into account their performance, we must mention the denoising systems proposed in [2] and [3]. The denoising system proposed in [2] is based on the shape-adaptive DCT (SA-DCT) transform that can be computed on a support of arbitrary shape. The SA-DCT is used in conjunction with the Anisotropic Local Polynomial Approximation (LPA) - Intersection of Confidence Intervals (ICI) technique, which defines the shape of the transform support in a pointwise adaptive manner. Since supports corresponding to different points are in general overlapping, the local estimates are averaged together using adaptive weights that depend on the region's statistics. The denoising system proposed in [3] is a MAP filter that acts in the spatial domain. It makes a different treatment of regions with different homogeneity degree. These regions can be treated independent with the same MAP filter choosing between different prior models. The multi-resolution analysis performed by the WT has been shown to be a powerful tool to achieve good denoising. In the wavelet domain, the noise is uniformly spread throughout the coefficients, while most of the image information is concentrated in the few largest ones (sparsity of the wavelet representation), [4-7]. The corresponding denoising methods have three steps, [1]: 1) The computation of the forward WT, 2) the filtering of the wavelet coefficients, 3) the computation of the IWT of the result obtained. Numerous WTs can be used to operate these treatments. The first one was the Discrete Wavelet Transform, DWT, [1]. It has three main disadvantages, [8]: lack of shift invariance, lack of symmetry of the mother wavelets and poor directional selectivity. These disadvantages can be diminished using a complex wavelet transform [8, 9]. Over twenty years ago, Grossman and Morlet [10] developed the Continuous Wavelet Transform (CWT) [11], using continuous complex-valued mother wavelets. Initial analysis based on wavelet decompositions was implemented using such mother wavelets. Both magnitude and phase descriptions of non-stationary signals were determined, and an early example of analysis includes wavelet ridge methods proposed by Delprat *et al.* [12]. However subsequently for many years interest focused on the Discrete Wavelet Transform (DWT) and signal estimation. The DWT was developed to implement the

WT of time-compact mother wavelets and as compact discrete wavelet filters cannot be exactly analytic [13], real wavelets were used. A revival of interest in later years has occurred in both signal processing and statistics for the usage of complex wavelets, [14], and in particular complex analytic wavelets [15]–[17]. This revival of interest may be linked to the development of complex-valued discrete wavelet filters [18] and the clever dual filter bank [15, 19]. The complex wavelet transform has been shown to provide a powerful tool in signal and image analysis [11], where most of the properties of the transform follow from the analyticity of the wavelet function. In [20] were derived large classes of wavelets generalizing the concept of a 1-D local complex-valued analytic decomposition to a 2-D vector-valued hyperanalytic decomposition. In the present paper we propose the utilization of a very simple implementation of the HWT, recently proposed, [21]. It has a high shift-invariance degree versus other quasi-shift-invariant WTs at same redundancy. It has also an enhanced directional selectivity. All the WTs have two parameters: the mother wavelets, MW and the primary resolution, PR, (number of iterations). The importance of their selection is highlighted in [23]. Another appealing particularity of those transforms, coming from their multiresolution capability, is the interscale dependency of the wavelet coefficients. Numerous non-linear filter types can be used in the WT domain. A possible classification is based on the nature of the useful component of the image to be processed. Basically, there are two categories of filters: those built assuming knowledge of noise statistics, only, and those based on knowledge of both signal and noise statistics. To the first category belong the hard-thresholding filter, [1], the soft-thresholding filter, [1,11], that minimizes the Min-Max estimation error and the Efficient SURE-Based Inter-scales Pointwise Thresholding filter [24], that minimizes the Mean Square Error, (MSE). Filters obtained by minimizing a Bayesian risk under a cost function, typically a delta cost function (MAP estimation [4,5,7]) or the minimum mean squared error (MMSE estimation [6]), belong to the second category. The construction of MAP filters supposes the existence of two statistical models, for the useful component of the input image and for its noise component. The MAP estimation of u, realized using the observation $y=u+n$, (where n represents the WT of the noise and u the WT of the useful component of the input image) is given by the following relation, called MAP filter equation:

$$\hat{u}(y) = \arg\max_{u}\left\{ln\left(f_n(y-u)\,f_u(u)\right)\right\} \qquad (1)$$

where f_x represents the probability density function (pdf) of x. Generally, the noise component is assumed Gaussian distributed. For the useful component there are many models. This distribution changes from scale to scale. For the first iterations of the WT it is a heavy tailed distribution. There are two solutions to deal with this mobility. The first one assumes to use a fixed simple model, risking an increase of inaccuracy across the scales. This way, there is a chance to obtain a closed form input-output relation for the MAP filter. This is the case of the bishrink filter [5]. An explicit input-output relationsheep has two advantages: it simplifies the implementation of the filter and it permits the analysis of its sensitivities. The second solution assumes to use a generalized model, defining a family of distributions and the identification of the best fitting element of this family for the distribution of the wavelet coefficients at a given scale. For example in [4] the family of Pearson's distributions is used, in [7] the family of SαS distributions and in [25] the model of Gauss–Markov random field. The use of such generalized model makes the treatment more accurate but implies implicit solutions for the MAP filter equation, which can often be solved only numerically and the sensitivities of the filter obtained cannot be evaluated. If the pdfs f_u and f_n do not take into account the interscale dependency of the wavelet coefficients than the MAP filter obtained is called marginal. This paper proposes a new denoising method for images based on the association of the new implementation of HWT, already mentioned, [21], with a very simple marginal MAP filter. The second section is dedicated to the new implementation of the HWT. The third section presents this marginal MAP filter. The aim of the fourth section is the presentation of some simulation results. The paper concludes with few final remarks.

II. A NEW IMPLEMENTATION OF THE HWT

The generalization of the analyticity concept in 2D is not obvious, because there are multiple definitions of the Hilbert transform in this case. In the following we will use the definition of the analytic signal associated to a 2D real signal named hypercomplex signal. So, the hypercomplex mother wavelet associated to the real mother wavelet $\psi(x,y)$ is defined as:

$$\begin{aligned}\psi_a(x,y) &= \psi(x,y) + i\mathcal{H}_x\left\{\psi(x,y)\right\} + \\ &+ j\mathcal{H}_y\left\{\psi(x,y)\right\} + k\mathcal{H}_x\left\{\mathcal{H}_y\left\{\psi(x,y)\right\}\right\}\end{aligned} \qquad (2)$$

where $i^2 = j^2 = -k^2 = -1,\ and\ ij = ji = k$, [22].

The HWT of the image $f(x,y)$ is:

$$HWT\left\{f(x,y)\right\} = \left\langle f(x,y), \psi_a(x,y)\right\rangle. \qquad (3)$$

Taking into account relation (2) it can be written:

$$\begin{aligned}&HWT\left\{f(x,y)\right\} = DWT\left\{f(x,y)\right\} + \\ &iDWT\left\{\mathcal{H}_x\left\{f(x,y)\right\}\right\} + jDWT\left\{\mathcal{H}_y\left\{f(x,y)\right\}\right\} + \\ &+kDWT\left\{\mathcal{H}_y\left\{\mathcal{H}_x\left\{f(x,y)\right\}\right\}\right\} = \\ &\left\langle f_a(x,y), \psi(x,y)\right\rangle = DWT\left\{f_a(x,y)\right\}.\end{aligned} \qquad (4)$$

So, the 2D-HWT of the image $f(x,y)$ can be computed with the aid of the 2D-DWT of its associated hypercomplex image. The new HWT implementation, [21], presented in figure 1, uses four trees, each one implementing a 2D-DWT. The first tree is applied to the input image. The second and

the third trees are applied to 1D discrete Hilbert transforms computed across the lines ($\mathcal{H}_x$) or columns ($\mathcal{H}_y$) of the input image. The fourth tree is applied to the result obtained after the computation of the two 1D discrete Hilbert transforms of the input image. The enhancement of the directional selectivity of the 2D-HWT is realized as in the case of the 2D-DTCWT, [9,19], by linear combinations of detail coefficients belonging to each subband of each of the four 2D DWTs. Let us consider, for example, the case of the diagonal detail subbands, (HH), presented in figure 2. We selected a particular input image, $f(x,y)=\delta(x,y)$, to appreciate the frequency responses associated to different transfer functions represented in figure 1. More precisely, the example in figure 2 refers to the transfer functions that relate the input f with the outputs z_{-r} and z_{+r}. The spectrum of the input image, $\mathcal{F}\{\delta(x,y)\}(f_x,f_y)$ is constant. The wavelet coefficients belonging to the subband HH are obtained by lines and columns high-pass filtering. We have assumed ideal high-pass filters. The spectra of the wavelet coefficients d_1, d_2, d_3, d_4 belonging to the subband HH, $\mathcal{F}\{DWT_{HH}\{\delta(x,y)\}\}$, $\mathcal{F}\{DWT_{HH}\{\mathcal{H}_x\{\delta(x,y)\}\}\}$, $\mathcal{F}\{DWT_{HH}\{\mathcal{H}_y\{\delta\}\}\}$, $\mathcal{F}\{DWT_{HH}\{\mathcal{H}_y\{\mathcal{H}_x\{\delta\}\}\}\}$, have two preferential orientations, corresponding to the two diagonals ($\pm\pi/4$). So, the 2D DWT cannot separate these two orientations. But the spectra of the coefficients obtained after linear combinations, for example z_{-r} and z_{+r}, $\mathcal{F}\{{}^{HH}z_{-r}\}(f_x,f_y)$ and $\mathcal{F}\{{}^{HH}z_{+r}\}(f_x,f_y)$, have only one preferential direction, the second diagonal respectively

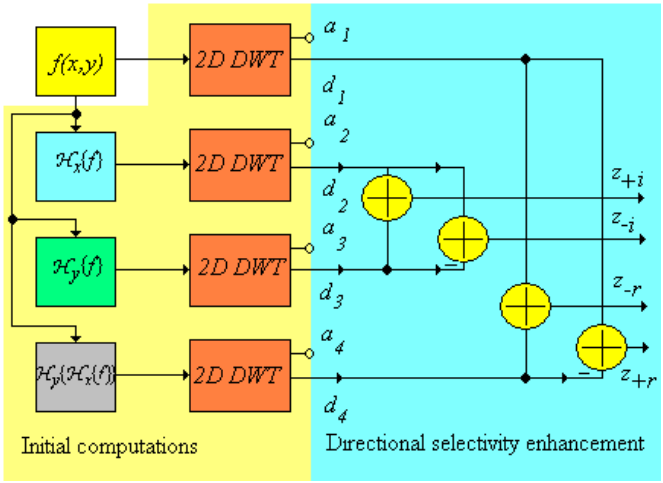

Figure 1. The new 2D-HWT-implementation architecture.

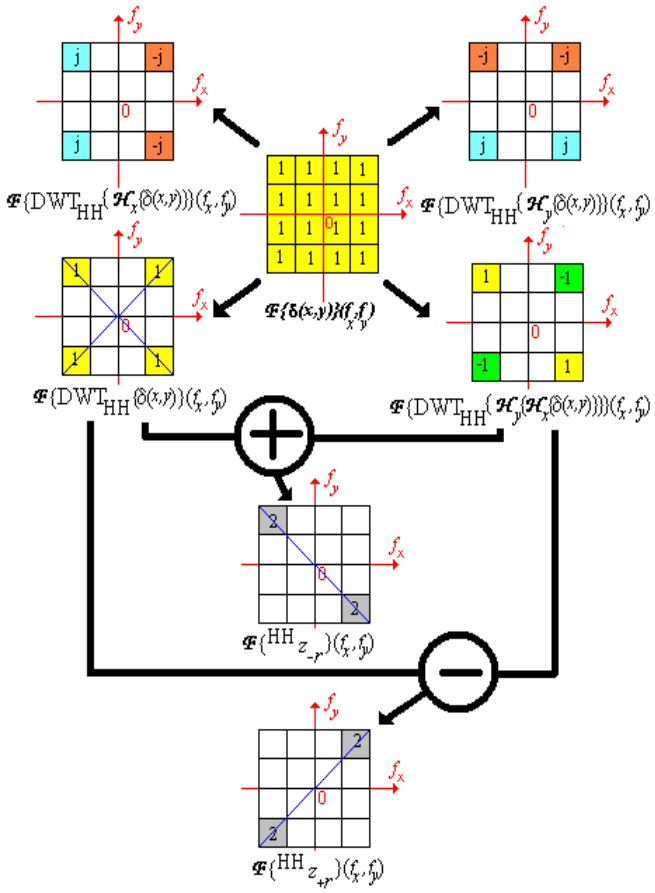

Figure 2. The strategy of directional selectivity enhancement in the HH subband. The frequency responses of the systems that transform the input image f into the output diagonal detail coefficient sub-images z_{-r} and z_{+r} represented in figure 1.

the first one. So, using the 2D HWT these directions can be separated. The same strategy can be used to enhance the directional selectivity in the other two subbands: LH and HL, obtaining the preferential orientations: $\pm\text{atan}(2)$ and $\pm\text{atan}(1/2)$. A comparison of the directional selectivity of the 2D DWT and the proposed implementation of the 2D HWT is presented in figure 3. We have conceived a special input image, in the frequency domain, to conduct this simulation. Its spectrum, represented in figure 3, is oriented following the directions: 0, $\pm\text{atan}(1/2)$, $\pm\pi/4$, $\pm\text{atan}(2)$ and π. The better directional selectivity of the new implementation of 2D-HWT versus the 2D-DWT can be easily observed. For example, the new implementation makes the difference between the two principal diagonals or between the directions $\pm\text{atan}(1/2)$ whereas the DWT cannot make such differences.

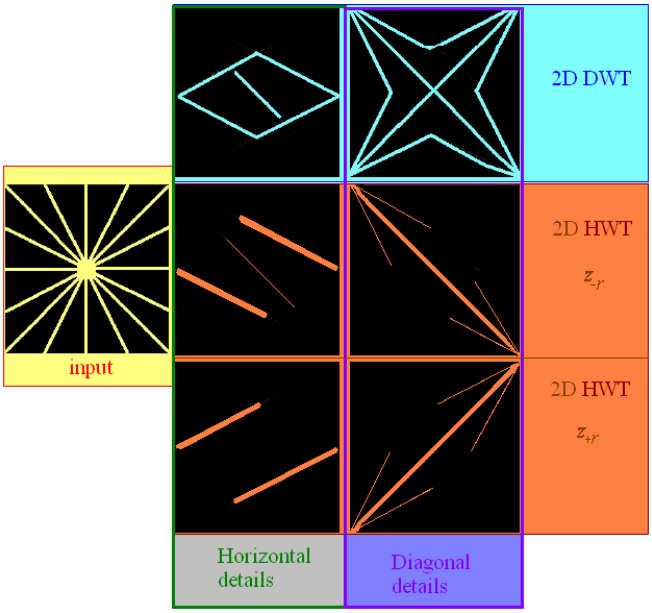

Figure 3. The absolute values of the spectra of horizontal and diagonal detail sub-images obtained after the first iterations of2D DWT and 2D HWT (proposed implementation). In the HWT case, the directional selectivity was enhanced using linear combinations.

III. THE MARGINAL MAP FILTER

In the following, we will consider a Gaussian distribution for the noise coefficients (f_n) and a Laplacian distribution for the useful signal coefficients (f_u). The noise coefficients have zero mean and variance σ_n^2. Regarding the a-priori statistical assumptions made, note that the wavelet transform of an image consists into a small number of high value wavelet coefficients (especially marking the contours) and a large number of small value coefficients (for the homogeneous regions). A heavy-tailed distribution for these coefficients seems therefore far more realistic than a Gaussian-one, and the particular case of a Laplacian pdf becomes attractive by its computational tractability.

A. The solution of the MAP filter equation

Consequently, we take:

$$f_u(u) = \frac{1}{\sqrt{2}\sigma_u} exp\left(-\frac{\sqrt{2}|u|}{\sigma_u}\right) \tag{5}$$

Under the considered hypothesis, the equation (1) becomes:

$$\frac{y-\hat{u}}{\sigma_n^2} - \frac{\sqrt{2}}{\sigma_u} sgn\,\hat{u} = 0. \tag{6}$$

Finally, the solution can be expressed as:

$$\hat{u} = sgn(y)\left(|y| - \sqrt{2}\sigma_n^2/\sigma_u\right)_+, \tag{7}$$

where $(X)_+ = X$ for $X>0$ and 0 otherwise. In the equation (7), we denote by σ_n^2 the noise variance and by σ_u the standard deviation of the useful image coefficients. The relation (7) reduces to a soft-thresholding of the noisy coefficients with a variable threshold. In practice, the statistical parameters in (7) are not known and therefore they must be estimated. To estimate the noise variance σ_n^2 from the noisy wavelet coefficients, a robust median estimator is used from the finest scale wavelet coefficients corresponding to each of the four DWTs:

$$\hat{\sigma}_n^2 = \frac{\text{median}\left(|y_i|\right)}{0.6745}, \quad y_i \in \text{subband HH}. \tag{8}$$

In [5], the marginal variance of the k'th coefficient is estimated using neighboring coefficients in the region $N(k)$, a window centered at the k'th coefficient. To make this estimation one gets $\sigma_y^2 = \sigma_u^2 + \sigma_n^2$, where σ_y^2 is the marginal variance of noisy observations, y. For the estimation of σ_y^2 is the following relationship is used:

$$\hat{\sigma}_y^2 = \frac{1}{M}\sum_{y_i \in N(k)} y_i^2, \tag{9}$$

where M is the size of the neighborhood $N(k)$. Then σ_u can be estimated as:

$$\hat{\sigma}_u = \sqrt{\left(\hat{\sigma}_y^2 - \hat{\sigma}_n^2\right)_+}. \tag{10}$$

B. Directional windows in wavelets domain

In [5] the regions $N(k)$ were rectangular with size 7x7. In [26] directional windows were proposed. The algorithm in [5] uses the same squared window for all the three oriented subbands in each level of a 2D DWT, which, in fact, imposes an assumption that the energy distribution of the image in each oriented subband is isotropic. However, this is not true for most images. The energy clusters in the horizontal, vertical, and diagonal subbands are mainly distributed along the horizontal, vertical, and diagonal directions, respectively. For this reason, the estimator using a squared window often leads to downward-biased estimates within and around energy clusters, which is disadvantageous to preserve the edges and texture in images. In [26], the elliptic directional windows are introduced to estimate the signal variances in each oriented subband. We generalized here this idea for the proposed implementation of the 2D HWT, using constant array elliptic estimation windows which have their principal axe oriented following the directions: $\pm\text{atan}(1/2)$, $\pm\pi/4$, and $\pm\text{atan}(2)$.

IV. SIMULATION RESULTS

In the following, some simulation results, obtained using the image Lena (size 512x512) additively perturbed with white Gaussian noise, are reported. First we have done a comparison between the associations HWT-proposed MAP filter and DWT-adaptive soft thresholding filter.

The mother wavelets used were Dau5, Dau7 and Dau10 (belonging to the Daubechies mother wavelets family and having the number of vanishing moments indicated). For the proposed MAP filter rectangular estimation windows with size 7x7 were used. The threshold was adaptively selected in the case of the second mentioned association to maximize the output peak signal to noise ratio, PSNR. The output PSNRs obtained using the proposed denoising method outperform the corresponding values obtained using the association DWT-adaptive soft thresholding with 3dB for any mother wavelet and noise level used. This gain can be attributed to the MAP filter. To highlight the advantages of the HWT versus the DWT in denoising, we have compared the contours treatment done by the two associations in the experiments already reported. In this respect, we have detected the contours of the useful component of the input image and of the denoising result and we have computed their mean square error. We have used the same mother wavelet, Dau4, and different noise levels. The results obtained are presented in table I. The case corresponding to the second line of the table is represented in figure 4. In the following we have compared the two types of estimation windows: rectangular and elliptic, proposed in this paper.

TABLE I. A COMPARISON OF THE CONTOURS TREATMENT REALIZED BY THE TWO DENOISING METHODS BASED ON THE HWT AND THE DWT (MEAN SQUARE ERRORS)

σ_n	HWT	DWT
10	0.0006	0.04
15	0.0007	0.0058
20	0.0015	0.0062
25	0.0035	0.0067
30	0.0044	0.0072
35	0.0055	0.0088

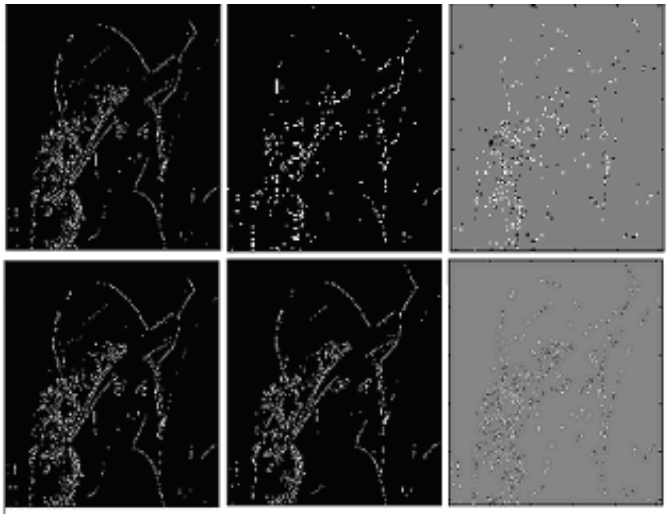

Figure 4. A comparison of the contours treatment realized by the two denoising method, based on the DWT (first line) and on the HWT (second line). On the first column are represented the contours of the useful component of the input image. On the second column are represented the contours of the two denoising results and on the third column the differences of the first two columns.

For the left-up corner of the image Lena of size 128x128, selected for his reach geometric content, we have proved that for any of the mother wavelets used and for any noise level, the output PSNR obtained using directional estimation windows is superior (with more than 2.5 dB) to the corresponding value obtained using rectangular estimation windows. This conclusion remains correct for the whole Lena image. In figure 5 are represented the input image (corresponding to an additive perturbation with white Gaussian noise having a standard deviation of σ_n=10) and the denoising results obtained using the two variants proposed in this paper and the mother wavelets Dau10. The value of the input PSNR is of 28.16 dB (figure 5, first image) and the values of the output PSNRs are of 32.52 dB for the variant corresponding to rectangular estimation windows (figure 5, second image) and of 34.09 dB for the variant corresponding to directional estimation windows (figure 5, third image).

Figure 5. A comparison of the results obtained using the two variants of the proposed denoising method. From up to bottom: the input image, the result obtained using rectangular windows and the result obtained using directional windows.

The directional treatment reduces the block effect on Lena's homogeneous areas and seems to enhance some directional features as the nose. In fact these results are comparable (slightly better) with the results obtained using another WT with enhanced directionality, the contourlet transform, reported in [27]. These results can be also compared with those reported in [28], where the filtering in the HWT domain is realized without MAP systems.

V. CONCLUSION

The HWT is a very modern WT as it has been formalized only one year ago [20]. It was already used in image processing, [28], the method obtained being named hyperanalytic denoising. In this paper we have used a very simple implementation of this transform, which permits the exploitation of the mathematical results and of the algorithms previously obtained in the evolution of wavelets theory. It does not require the construction of any special wavelet filter. It has a very flexible structure, as we can use any orthogonal or biorthogonal real mother wavelets for the computation of the HWT. Our simulation results are similar or better than the results obtained using other denoising methods based on new wavelet transforms, like for example the contourlet transform, [27]. The approach presented in this paper is different in comparison with the denoising strategy proposed in [28] from two points of view: the implementation of the 2D HWT and the filter used in the wavelets domain. We have preferred a MAP filter based on a very simple model of the wavelet coefficients of the useful image. We have compared two implementations of the MAP filter differing by the form and orientation of the windows used to estimate the local standard deviation of the useful image and we highlighted the superiority of directional windows.

The simulation results presented in this paper illustrate the effectiveness of the proposed algorithm. The comparisons made suggest the new denoising results are competitive with the best wavelet-based results reported in literature, despite the inaccuracy of the statistical model used.

ACKNOWLEDGMENT

The research with the results reported in this paper was realized in the framework of the Programme de recherche franco-roumain Brancusi with the title: Débruitage des images SONAR en utilisant la théorie des ondelettes.

REFERENCES

[1] D. L. Donoho, I. M. Johnstone, Ideal spatial adaptation by wavelet shrinkage, *Biometrika*, 81(3) : 425-455, 1994.

[2] Foi, A., V. Katkovnik, and K. Egiazarian, Pointwise Shape-Adaptive DCT for High-Quality Denoising and Deblocking of Grayscale and Color Images, (in review) *IEEE Trans. Image Process*., April 2006. (preprint).

[3] M. Walessa, M. Datcu, Model-Based Despeckling and Information Extraction from SAR Images, *IEEE Transactions on Geoscience and Remote Sensing*, vol. 38, no. 5, September 2000, 2258- 2269.

[4] Samuel Foucher, Gozie Bertin Benie, Jean-Marc Boucher, Multiscale MAP Filtering of SAR images, *IEEE Transactions on Image Processing*, vol. 10, no.1, January 2001, 49-60.

[5] L. Sendur and I. W. Selesnick, Bivariate shrinkage functions for wavelet-based denoising exploiting interscale dependency, *IEEE Trans. on Signal Processing*, 50(11): 2744-2756, November 2002.

[6] A. Pizurica, W. Philips, Estimating the probability of the presence of a signal of interest in multiresolution single and multiband image denoising, *IEEE Transactions on Image Process.* 15(3) (2006) 654-665.

[7] A. Achim and E. E. Kuruoglu, Image Denoising Using Bivariate α-Stable Distributions in the Complex Wavelet Domain, *IEEE Signal Processing Letters*, 12(1):17-20, January 2005.

[8] N. Kingsbury, Complex Wavelets for Shift Invariant Analysis and Filtering of Signals, *Applied and Comp. Harm. Anal.* 10, 2001, 234-253.

[9] N G Kingsbury, A Dual-Tree Complex Wavelet Transform with improved orthogonality and symmetry properties, *Proc. IEEE Conf. on Image Processing*, Vancouver, September 11-13, 2000, paper 1429.

[10] A. Grossman and J. Morlet, Decomposition of Hardy functions into square integrable wavelets of constant shape, *SIAM J. Math. Anal.*, vol. 15, pp. 723–736, 1984.

[11] S. Mallat, A Wavelet Tour of Signal Processing, 2nd Edition, *Academic Press*, New York, 1999.

[12] N. Delprat, B. Escudié, P. Guillemain, R. Kronland-Martinet, Ph. Tchamitchian, and B. Torresani, Asymptotic wavelet and Gabor analysis: Extraction of instantaneous frequencies, *IEEE Trans. Inform. Theory*, vol. 38, pp. 644–64, 1992.

[13] P. Auscher, Il n'existe pas de bases d'ondelettes regulieres dans l'espace Hardy $h^2(\backslash)$, *C. R. Acad Sci Paris*, vol. 315, pp. 769–72, 1992.

[14] S. Barber and G. P. Nason, Real nonparametric regression using complex wavelets, *J. Roy. Stat. Soc. B*, vol. 66, pp. 927–939, 2004.

[15] N. G. Kingsbury, Image processing with complex wavelets, *Philosophical Transactions of the Royal Society of London A*, vol. 357, pp. 2543 – 2560, 1999.

[16] I. W. Selesnick, The design of approximate Hilbert transform pairs of wavelet bases, *IEEE Trans. on Signal Processing*, vol. 50, pp. 1144–1152, 2002.

[17] I. W. Selesnick, Hilbert transform pairs of wavelet bases, *IEEE Signal Processing Letters*, vol. 8, pp. 170–173, 2001.

[18] J.-M. Lina and M. Mayrand, Complex daubechies wavelets, *Applied and Computational Harmonic Analysis*, vol. 2, pp. 219–229, 1995.

[19] I. W. Selesnick, R. G. Baraniuk, and N. G. Kingsbury, The dual-tree complex wavelet transform, *IEEE Signal Processing Magazine*, vol. 22(6), pp. 123–51, 2005.

[20] S. C. Olhede, Georgios Metikas, The Hyperanalytic Wavelet Transform, *Imperial College Statistics Section* Technical Report TR-06-02, May 23, 2006.

[21] I. Adam, C. Nafornita, J-M Boucher, A. Isar, A New Implementation of the Hyperanalytic Wavelet Transform, paper acccepted at *ISSCS 2007*, Iasi, Romania, in press.

[22] C. Davenport, Commutative Hypercomplex Mathematics, http://home.usit.net/~cmdaven/cmdaven1.htm

[23] G.P. Nason, Choice of wavelet smoothness, primary resolution and threshold in wavelet shrinkage, *Statistics and Computing*, 12, 2002, 219-227.

[24] F. Luisier, T. Blu, M. Unser, A New SURE Approach to Image Denoising: Inter-Scale Orthonormal Wavelet Thresholding, *IEEE Transactions on Image Processing*, in press.

[25] D. Gleich, M. Datcu, Gauss–Markov Model for Wavelet-Based SAR Image Despeckling, *IEEE Sig. Proc. Let.*, vol. 13, no. 6, June 2006, 365-368.

[26] Peng-Lang Shui, Image Denoising Algorithm via Doubly Local Wiener Filtering With Directional Windows in Wavelet Domain, *IEEE Sig. Proc. Let.*, Vol. 12, No. 6, October 2005, 681-684.

[27] Duncan D.-Y. Po and Minh N. Do, Directional Multiscale Modeling of Images using the Contourlet Transform, *IEEE Workshop on Statistical Signal Processing*, Oct. 2003, 262 – 265.

[28] Sofia C. Olhede, Hyperanalytic Denoising, *Imperial College Statistics Section* Technical Report TR-06-01 1, Department of Mathematics, Imperial College London, SW7 2AZ UK.